JAMECH

Vol. 46, No. 1, January. 2015, pp 77- 91

3-node Basic Displacement Functions in Analysis of Non-Prismatic Beams

A. Modarakar Haghighi [1*], M. Zakeri [1], R. Attarnejad [1,2]

1. School of Civil Engineering, College of Engineering, University of Tehran, Tehran P.O. Box 11365-4563, Iran

2. Centre of Numerical Methods in Engineering, University of Tehran, Tehran, Iran

Received 1 October 2014; Accepted 11 March 2015

Abstract

Purpose– Analysis of non-prismatic beams has been focused of attention due to wide use in complex structures such as aircraft, turbine blades and space vehicles. Apart from aesthetic aspect, optimization of strength and weight is achieved in use of this type of structures. The purpose of this paper is to present new shape functions, namely 3-node Basic Displacement Functions (BDFs) for derivation of structural matrices for general non-prismatic Euler-Bernoulli beam elements. Design/methodology/approach– Static analysis and free transverse vibration of non-prismatic beams are extracted studied from a mechanical point of view. Following structural/mechanical principles, new static shape functions are in terms of BDFs, which are obtained using unit-dummy-load method. All types of cross-sections and cross-sectional dimensions of the beam element could be considered in this method. Findings– According to the outcome of static analysis, it is verified that exact results are obtained by applying one or a few elements. Furthermore, it is observed that results from both static and free transverse vibration analysis are in good agreement with the previous published once in the literature. Research limitations/implications– The method can be extended to structural analysis of curved and Timoshenko beams as well as plates and shells. Furthermore, exact dynamic shape functions can be derived using BDFs by solving the governing equation for transverse vibration of beams. Originality/value– The present investigation introduces new shape functions, namely 3-node Basic Displacement Functions (BDFs) extended from 2-node functions, and then compares its performance with previous element.

Keywords: *3-node basic displacement functions, free transverse vibration, non-prismatic beam, shape functions, static analysis.*

1. Introduction

Analysis of beams has been focused of attention due to wide use in complex structures such as aircraft, turbine blades and space vehicles. Apart from aesthetic aspect, optimization of strength and weight is achieved in use of this type of structures. Consequently, exact static and dynamic analyses of these members become more significant. Through the years, many researchers devoted their contributions to either formulating new

[*] Corresponding Author, Tel.: +98 9127935898; Fax: +98 21 22323705, Email:: za57190@gmail.com

elements or enhancing the existing approximate elements. Gunda and Ganguli [1] proposed new rational shape functions for finite-element analysis of rotating tapered beams through solving the static part of the governing differential equation.

Caruntu [2] utilized hyper-geometric functions to study free vibration of cantilever beams with parabolic thickness variation. Gallagher and Lee [3] derived approximate structural matrices for dynamic and instability analyses of non-uniform beams. Karabalis and Beskos [4] proposed a new element for static, stability and dynamic analyses of linearly tapered beams. Their method employs exact flexural and axial stiffness matrices but approximate consistent mass and geometric stiffness matrices. Eisenberger and Reich [5] obtained an approximate stiffness matrix for beams whose depth or width varied as an overall polynomial along beam length using shape functions of uniform beams.

Subsequently, Eisenberger [6, 7] derived exact stiffness matrices for beams with general variation of depth/width via a series solution of the governing equation. Banerjee and Williams [8] obtained exact dynamic stiffness matrix in terms of Bessel's functions for a class of tapered members whose area and moment of inertia vary as any arbitrary integer powers n and n+2, respectively. Mou et al. [9] computed the exact dynamic stiffness matrix in terms of hyper geometric functions for beams whose area and moment of inertia vary in accordance with any two arbitrary real-number powers.

Studying the effects of reduced beam section frame elements on stiffness of moment frames, Chambers et al. [10] derived stiffness matrix of a two-dimensional frame element with radius flange reductions, which is symmetric about the centroid of the element using virtual work theories. Kim and Engelhardt [11] proposed a new non-prismatic beam element for modeling the elastic behavior of steel beams with reduced beam section connections. Ece et al. [12] performed vibration analysis by analytical solving of governing differential equation of free vibration of beams with exponentially varying width and constant height.

In recent years, several researchers have focused on vibration of non-prismatic beams by solving the governing equation of motion via application of different numerical techniques, i.e. Frobenius method [13-15], Chebyshev series [16], Raleigh-Ritz method [17] and differential transform method [18-28]. The analysis of structural members generally includes two methods, namely displacement-based method (stiffness method) and flexibility method (force method). Equilibrium of forces, compatibility of displacements/strains and constitutive law of materials are the basic three essential relations that should be satisfied for the exact solution in any structural analysis. Additionally, an extra hypothesis in the displacement field is usually imposed in addition to these three fundamental relations. Generally, the equilibrium equations are satisfied only in certain points of elements, such as integration points. Thus the stiffness method is approximate in nature; however, the generality of this method seems to be the great advantage. In contrary, the flexibility method ensures accurate structural analysis and satisfies the equilibrium equations at any interior point of the element. However, the application of this method usually requires complicated and tedious calculations.

In this study, a simple flexibility-based formulation is proposed for derivation of structural matrices for general non-prismatic Euler-Bernoulli beam elements. This concept was, firstly, proposed by Attarnejad [29-31]. Basic Displacement Functions (BDFs) are presented; and 3-node method is introduced extending from 2-node method. Exact shape functions are obtained from these BDFs. There are two categories of BDFs, namely static BDFs, which are derived based on static deformations [31-33] and dynamic BDFs, which are derived assuming dynamic deformations [34-37]. The BDFs presented are obtained on the basis of static deformations. The advantage of this method is that it does not involve any cumbersome mathematical/numerical calculation; it also covers most of the engineering problems concerning non-prismatic beams.

The basic elements of a paper in the order in which they should appear are: Title, Authors, Affiliations, Abstract, Keywords, Main text, Acknowledgments, Appendix, and References. Authors should submit their manuscript by the Journal website. Electronic submission substantially reduces the editorial processing, reviewing and publication times. Please attach your covering letter providing assurance that the manuscript has neither been published nor submitted for publication elsewhere. The corresponding author will be noted of the acceptance of their paper by the editor.

The authors of accepted paper with conditional acceptance are required to address the comments of the referees suitably in their revised paper and in their final full paper and address their revisions properly in a separate file and upload it to the Journal website. Authors will be asked, upon acceptance of an article, to transfer copyright of the article to the publisher. This will ensure the widest possible dissemination of the information under copyright laws. This form can be uploading from the Journal website. The Editors reserve the right to return manuscripts that do not conform to the instructions for manuscripts preparation or papers that do not fit the scope Journal, prior to referring.

2. Basic Displacement Functions

BDFs are mathematical functions, which derived from fundamental mechanical concepts. For definition of BDFs, consider a beam which one of its nodes is free; the others are clamped. A BDFs is defined as nodal displacement of the free node due to unit load at the distance x. For a 3-node beam, BDFs are introduced as:

b_{wm} : vertical displacement of the m-th node due to unit load at distance x when the beam is clamped at the others.

$b_{\theta m}$: angle of rotation of the m-th node due to unit load at distance x when the beam is clamped at the others.

(where m=1, 2, 3)

$b_{w1}, b_{\theta 1}, b_{w2}, b_{\theta 2}, b_{w3}, b_{\theta 3}$ are showed in Figure 1.

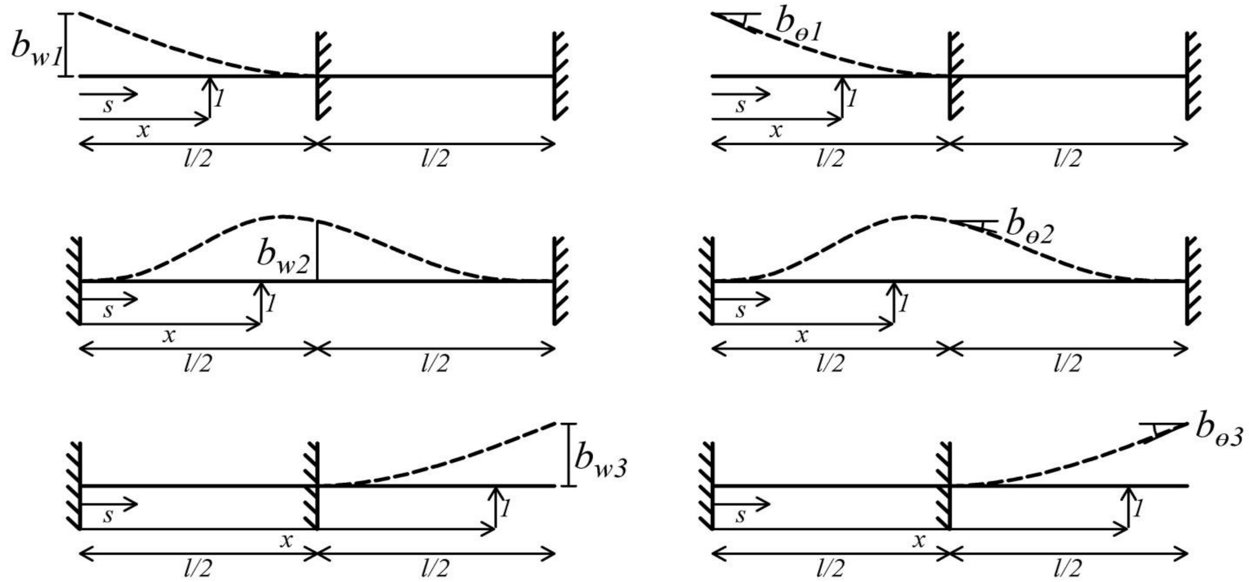

Fig. 1. Definitions of BDFs

For 1st and 3th nodes:

$$b_{w1}(x) = sg(\frac{l}{2} - x)\int_x^{l/2} \frac{s(s-x)}{EI(s)} ds \tag{1}$$

$$b_{\theta 1}(x) = sg(\frac{l}{2} - x)\int_x^{l/2} \frac{-(s-x)}{EI(s)} ds \tag{2}$$

$$b_{w3}(x) = sg(x - \frac{l}{2})\int_{l/2}^{x} \frac{(l-s)(x-s)}{EI(s)} ds \tag{3}$$

$$b_{\theta 3} = sg(x - \frac{l}{2})\int_{l/2}^{x} \frac{-(s-x)}{EI(s)} ds \tag{4}$$

where:

$$sg(y) = \begin{cases} 0 & y < 0 \\ 1 & y \geq 0 \end{cases}$$

For the mid-node:

By solving the geometry equations, reactions are determined due to unit load at distance x (Fig. 2):

$$R_1 = \frac{\int_x^l \frac{s\left(s-x\right)}{EI(s)} ds \int_0^l \frac{1}{EI(s)} ds - \int_x^l \frac{\left(s-x\right)}{EI(s)} ds \int_0^l \frac{s}{EI(s)} ds}{\int_0^l \frac{s^2}{EI(s)} ds \int_0^l \frac{1}{EI(s)} ds - \int_0^l \frac{s}{EI(s)} ds \int_0^l \frac{s}{EI(s)} ds} \tag{5}$$

$$M_1 = \frac{\int_x^l \frac{\left(s-x\right)}{EI(s)} ds \int_0^l \frac{s^2}{EI(s)} ds - \int_x^l \frac{s\left(s-x\right)}{EI(s)} ds \int_0^l \frac{s}{EI(s)} ds}{\int_0^l \frac{s}{EI(s)} ds \int_0^l \frac{s}{EI(s)} ds - \int_0^l \frac{s^2}{EI(s)} ds \int_0^l \frac{1}{EI(s)} ds} \tag{6}$$

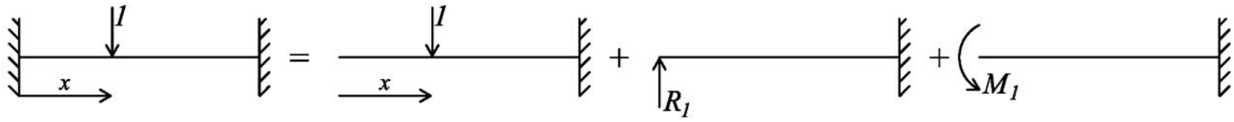

Fig. 2. General beam with unit load at distance x decomposed into isostatic structures

which moment through the beam can be obtained:

$$M_s = R_1 s - M_1 - H(s-x)\left(s-x\right) \tag{7}$$

Following similar procedure, we can obtain support reactions due to unit load and unit moment at distance $l/2$ (Fig. 3).

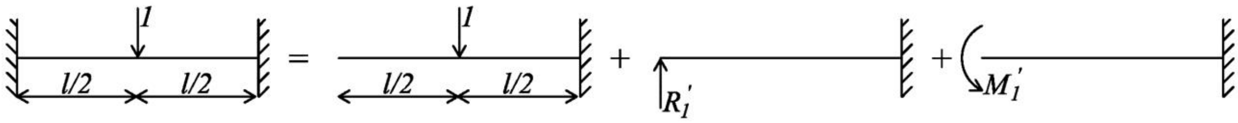

Fig. 3. General beam with unit load at distance $l/2$ divided into isostatic structures

$$R_1' = \frac{\int_{l/2}^l \frac{s\left(s-\frac{l}{2}\right)}{EI(s)} ds \int_0^l \frac{1}{EI(s)} ds - \int_{l/2}^l \frac{\left(s-\frac{l}{2}\right)}{EI(s)} ds \int_0^l \frac{s}{EI(s)} ds}{\int_0^l \frac{s^2}{EI(s)} ds \int_0^l \frac{1}{EI(s)} ds - \int_0^l \frac{s}{EI(s)} ds \int_0^l \frac{s}{EI(s)} ds} \tag{8}$$

$$M_1' = \frac{\int_{l/2}^l \frac{\left(s-\frac{l}{2}\right)}{EI(s)} ds \int_0^l \frac{s^2}{EI(s)} ds - \int_{l/2}^l \frac{s\left(s-\frac{l}{2}\right)}{EI(s)} ds \int_0^l \frac{s}{EI(s)} ds}{\int_0^l \frac{s}{EI(s)} ds \int_0^l \frac{s}{EI(s)} ds - \int_0^l \frac{s^2}{EI(s)} ds \int_0^l \frac{1}{EI(s)} ds} \tag{9}$$

$$M_s' = R_1' s - M_1' - H\left(s-\frac{l}{2}\right)\left(s-\frac{l}{2}\right) \tag{10}$$

For unit moment (Fig. 4):

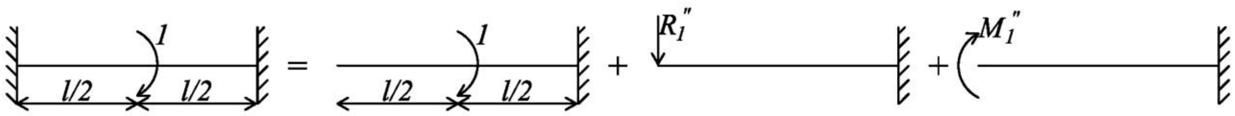

Fig. 4. General beam with unit moment at distance $l/2$ divided into isostatic structures

$$R_1'' = \frac{\int_{l/2}^l \frac{s}{EI(s)} ds \int_0^l \frac{1}{EI(s)} ds - \int_{l/2}^l \frac{1}{EI(s)} ds \int_0^l \frac{s}{EI(s)} ds}{\int_0^l \frac{s^2}{EI(s)} ds \int_0^l \frac{1}{EI(s)} ds - \int_0^l \frac{s}{EI(s)} ds \int_0^l \frac{s}{EI(s)} ds} \tag{11}$$

$$M_1'' = \frac{\int_{l/2}^{l}\frac{1}{EI(s)}ds\int_0^l\frac{s^2}{EI(s)}ds - \int_{l/2}^{l}\frac{s}{EI(s)}ds\int_0^l\frac{s}{EI(s)}ds}{\int_0^l\frac{s}{EI(s)}ds\int_0^l\frac{s}{EI(s)}ds - \int_0^l\frac{s^2}{EI(s)}ds\int_0^l\frac{1}{EI(s)}ds} \tag{12}$$

$$M_s'' = M_1'' - R_1''s + H(s-\frac{l}{2}) \tag{13}$$

Finally BDFs of the mid-node are:

$$b_{w2} = \int_0^l \frac{M_s M_s'}{EI(s)}ds \tag{14}$$

$$b_{\theta 2}(x) = \int_0^l \frac{M_s M_s''}{EI(s)}ds \tag{15}$$

Regarding the reciprocal theorem, each BDF has equivalent definitions, which are as follows:

b_{wm}: vertical displacement of a point at distance x due to unit load at the m-th node when the beam is clamped at the others.

$b_{\theta m}$: angle of rotation of a point at distance x due to unit moment at the m-th node when the beam is clamped at the others.

$b_{w1}, b_{\theta 1}, b_{w2}, b_{\theta 2}, b_{w3}, b_{\theta 3}$ are showed in Figure 5.

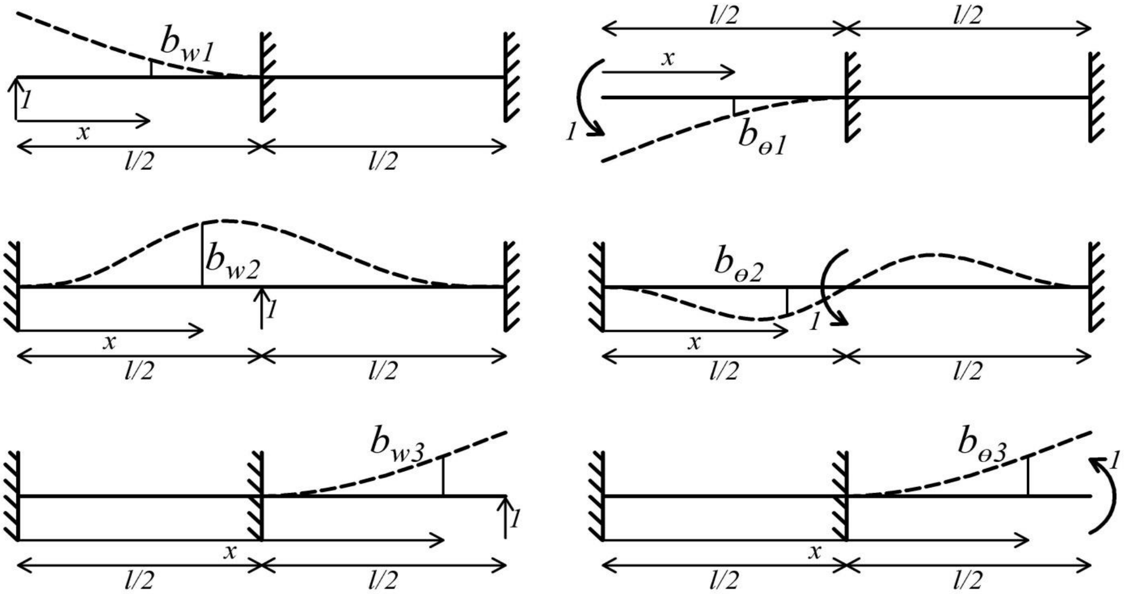

Fig. 5. Equivalent definitions of BDFs

Considering the equivalent definitions of BDFs, the angles of rotation and curvature of the beam corresponding to the BDF are respectively indicated in the first and second derivatives of each BDF. The required derivatives could be either obtained using principle of structural analysis or calculated using the Leibniz formula:

$$\frac{\partial}{\partial s}\int_{f_1(s)}^{f_2(s)} g(s,t)dt = \int_{f_1(s)}^{f_2(s)}\frac{\partial g(s,t)}{\partial s}dt + \frac{\partial f_2(s)}{\partial s}g(s,f_2(s)) - \frac{\partial f_1(s)}{\partial s}g(s,f_1(s))$$

Moreover, the flexibility matrix is obtained as:

$$F_{11} = \begin{bmatrix} b_{w1}(0) & b_{\theta 1}(0) \\ \left.\frac{db_{w1}}{dx}\right|_{x=0} & \left.\frac{db_{\theta 1}}{dx}\right|_{x=0} \end{bmatrix} \tag{16}$$

$$F_{22} = \begin{bmatrix} b_{w2}(\frac{l}{2}) & b_{\theta 2}(\frac{l}{2}) \\ \left.\frac{db_{w2}}{dx}\right|_{x=\frac{l}{2}} & \left.\frac{db_{\theta 2}}{dx}\right|_{x=\frac{l}{2}} \end{bmatrix} \tag{17}$$

$$\mathrm{F}_{33}=\begin{bmatrix} b_{w3}(l) & b_{\theta 3}(l) \\ \left.\dfrac{db_{w3}}{dx}\right|_{x=l} & \left.\dfrac{db_{\theta 3}}{dx}\right|_{x=l} \end{bmatrix} \tag{18}$$

The Nodal stiffness matrix can be obtained by inverting the nodal flexibility matrix.

3. Shape Function

Divide the structure of a general tapered beam subjected to external loading and is clamped at first, middle and end into two structures as shown in Figure 6.

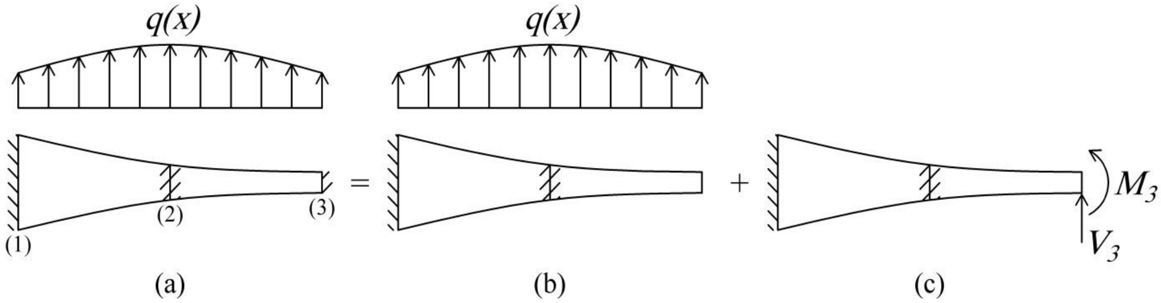

Fig. 6. General non-prismatic beams divided into two structure (b) and (c)

In structure (b), with regard to BDFs definitions, nodal displacement of point (3) due to external load can be calculated as followed:

$$\begin{Bmatrix} w_3 \\ \theta_3 \end{Bmatrix}^{(b)}=\int_l q(x)\begin{Bmatrix} b_{v3} \\ b_{\theta 3} \end{Bmatrix}dx \tag{19}$$

In structure (c), nodal displacement of point (3) can be calculated using flexibility matrix that:

$$\begin{Bmatrix} w_3 \\ \theta_3 \end{Bmatrix}^{(c)}=\mathbf{F_{33}}\begin{Bmatrix} V_3 \\ M_3 \end{Bmatrix} \tag{20}$$

By imposing the boundary conditions for displacement of point (3) we have:

$$\begin{Bmatrix} w_3 \\ \theta_3 \end{Bmatrix}=\begin{Bmatrix} w_3 \\ \theta_3 \end{Bmatrix}^{(b)}+\begin{Bmatrix} w_3 \\ \theta_3 \end{Bmatrix}^{(c)}=\begin{Bmatrix} 0 \\ 0 \end{Bmatrix} \tag{21}$$

Substituting equations (19) and (20) into equation (21) the reactions at point 3 are obtained as:

$$\begin{Bmatrix} V_3 \\ M_3 \end{Bmatrix}=-\mathbf{K_{33}}\int_l q(x)\begin{Bmatrix} b_{w3} \\ b_{\theta 3} \end{Bmatrix}dx \tag{22}$$

Following similar procedure, the reactions at points (1) and (2) are obtained:

$$\begin{Bmatrix} V_1 \\ M_1 \end{Bmatrix}=-\mathbf{K}_{11}\int_l q(x)\begin{Bmatrix} b_{w1} \\ b_{\theta 1} \end{Bmatrix}dx \tag{23}$$

$$\begin{Bmatrix} V_2 \\ M_2 \end{Bmatrix}=-\mathbf{K}_{22}\int_l q(x)\begin{Bmatrix} b_{w2} \\ b_{\theta 2} \end{Bmatrix}dx \tag{24}$$

The nodal equivalent loads which are the equal and opposite response to reactions are obtained as:

$$\mathbf{F}=\mathbf{G}\int_l q(x)\mathbf{b}dx \tag{25}$$

where b is a vector containing BDFs ($\mathrm{b}^T=\{b_{w1} \quad b_{\theta 1} \quad b_{w2} \quad b_{\theta 2} \quad b_{w3} \quad b_{\theta 3}\}$).
in which:

$$\mathbf{G}=\begin{bmatrix} \mathbf{K_{11}} & & \\ & \mathbf{K}_{22} & \\ & & \mathbf{K}_{33} \end{bmatrix} \tag{26}$$

Employing work-equivalent load method, nodal forces are given as:

$$\mathbf{F}=\int_l q(x)\mathbf{N}^T dx \tag{27}$$

Shape functions can be obtained by comparing equations (25) and (27):

$$\mathbf{N}=\mathbf{b}^T.\mathbf{G} \tag{28}$$

Therefore, structural matrices, i.e. stiffness and consistent mass matrices are given as (Gallagher and Lee [3]):

$$\mathbf{M}=\int_l \mathbf{N}^T \rho A(x)\mathbf{N}dx \tag{29}$$

$$\mathbf{K}=\int_l \mathbf{N}''^T EI(x)\mathbf{N}''dx \tag{30}$$

The structural matrices in terms of BDFs can be expressed using equations (28-30):

$$\mathbf{M}=\mathbf{G}(\int_{l}\mathbf{b}\rho A(x)\mathbf{b}^{T}dx)\mathbf{G} \quad (31)$$

$$\mathbf{K}=\mathbf{G}(\int_{l}\mathbf{b}''EI(x)\mathbf{b}''^{T}dx)\mathbf{G} \quad (32)$$

The application of BDFs can be clarified using a general algorithm for derivation of shape functions and structural matrices for non-prismatic beams in which each step is performed at unit length with constant cross-sectional area and moment of inertia. Obtaining BDFs using Equations (1-4) and (14-15):

$$b_{w1}=sg(0.5-x)\frac{(x+1)(2x-1)^2}{24EI}$$

$$b_{\theta 1}=sg(0.5-x)\frac{-(2x-1)^2}{8EI}$$

$$b_{w2}=sg(0.5-x)\frac{(3-4x)x^2}{48EI}$$

$$b_{\theta 2}=sg(0.5-x)\frac{x^2(2x-1)^2}{8EI}$$

$$b_{w3}=sg(x-0.5)\frac{-(x-2)(2x-1)^2}{24EI}$$

$$b_{\theta 3}=sg(x-0.5)\frac{(2x-1)^2}{8EI}$$

The first and second derivatives of BDFs.

Derivation of nodal flexibility matrices using Equations (16-18):

$$\mathbf{F_{11}}=\frac{1}{EI}\begin{bmatrix}0.0417 & -0.125\\ -0.125 & 0.5\end{bmatrix}$$

$$\mathbf{F}_{22}=\frac{1}{EI}\begin{bmatrix}0.0052 & 0\\ 0 & 0.0625\end{bmatrix}$$

$$\mathbf{F}_{33}=\frac{1}{EI}\begin{bmatrix}0.0417 & 0.125\\ 0.125 & 0.5\end{bmatrix}$$

Evaluating G using equation (29):

$$\mathbf{G}=EI\begin{bmatrix}96 & 24 & 0 & 0 & 0 & 0\\ 24 & 8 & 0 & 0 & 0 & 0\\ 0 & 0 & 192 & 0 & 0 & 0\\ 0 & 0 & 0 & 16 & 0 & 0\\ 0 & 0 & 0 & 0 & 96 & -24\\ 0 & 0 & 0 & 0 & -24 & 8\end{bmatrix}$$

Derivation of shape functions using Equation (28):

$$N_1=sg(0.5-x)(16x^3-12x^2+1)$$
$$N_2=sg(0.5-x)(4x^3-4x^2+x)$$
$$N_3=H(0.5-x)4(3-4x)x^2+H(0.5-x)(16x^3-36x^2+24x-4)$$
$$N_4=H(0.5-x)2(2x-1)x^2+H(0.5-x)(4x^3-10x^2+8x-2)$$
$$N_5=sg(x-0.5)(-16x^3+36x^2-24x+5)$$
$$N_6=sg(x-0.5)(4x^3-8x^2+5x-1)$$

where Heaviside step function ($H(x)$) is introduced in Appendix A.

Derivation of structural matrices using Equations (31) and (32):

$$\mathrm{K}=EI\begin{bmatrix}96 & 24 & -96 & 24 & 0 & 0\\ & 8 & -24 & 4 & 0 & 0\\ & & 192 & 0 & -96 & 24\\ & & & 16 & -24 & 4\\ & & & & 96 & -24\\ sym. & & & & & 8\end{bmatrix}$$

$$\mathrm{M}=EI\begin{bmatrix}0.1857 & 0.0131 & 0.0643 & -0.0077 & 0 & 0\\ & 0.0012 & 0.0077 & -0.0009 & 0 & 0\\ & & 0.3714 & 0 & 0.0643 & -0.0077\\ & & & 0.0024 & 0.0077 & -0.0009\\ & & & & 0.1857 & -0.0131\\ sym. & & & & & 0.0012\end{bmatrix}$$

4. Numerical Results and Discussions

In the present research, two types of numeric examples, including static analysis and free lateral vibration are discussed. The Gauss quadrature rule with 10 gauss points is used as a Numerical Integration technique. In order to describe boundary conditions, the symbolism C, S and F are utilized to identify the clamped, simply supported and free boundary conditions respectively. Except for static analysis, a uniform unit length beam is used for all numerical examples. The dimensionless natural frequency parameter, μ, is used to make comparisons between the results. μ_i is defined as follows:

$$\mu_i=\omega\sqrt{\frac{\rho_0 A_0 l^4}{E_0 I_0}}$$

4.1. Static analysis

Three different cantilever beams, in which $L=10m$, $E=3\times10^{8} kg.m$ are assumed and subjected to uniform load, $q=1000kg.m^{-1}$; Vertical deflection of free the end of each case is calculated and then compared with the results obtained from classical and non-classical methods [38]. The results are tabulated in Table 1.

Table 1. Deflection of tip due to distributed load 10^5 N/m

Case	Present	Franciosi and Mecca [38]						
		Non-classical				classical		
	NE=1	NE=1	NE =2	NE =5	NE =3	NE =10	NE =100	NE =200
A	3.157147	3.15715	3.15715	3.15715	3.28569	3.16841	3.15726	3.157176
B	1.543083	1.54308	1.54308	1.54308	1.8435	1.56832	1.54333	1.543145
C	2.414213	2.41424	2.41422	2.41421	2.99927	2.46085	2.414674	2.414329

The comparison shows that using the present method is more efficient in the static analysis. The three different cantilever beam cases are specified as follows:

Case A) unit depth, width is defined as:

$$b=2-0.175x$$

Case B) unit width, depth is defined as:

$$h=2-0.175x$$

Case C) unit width, depth is defined as:

$$h=\left(\sqrt{2}+(0.05-0.1\sqrt{2})x\right)^2$$

The vertical displacement is obtained using a single finite element with varying cross section and is reported in the second column.

4.2. Free lateral vibration

Example 1.

Consider a cantilever beam, in which the cross-section and moment of inertia vary as follows:

$$A(\xi)=A_0(1-c\xi)^n$$

$$I(\xi)=I_0(1-c\xi)^{n+2}$$

where $\xi=x/L$

Different values of n indicate the distinctive applications of the beam. For example, when n is set to two, the beam is applicable for beams with circular cross-section whose diameter varies linearly or for beams whose height and breadth both vary linearly with the same taper Raito. In order to investigate the efficiency of the method, the first three natural frequencies and special cases of $n=1$ and $n=2$ are compared with those of Banerjee *et al.* [15] and Attarnejad [31]. The results are tabulated in Table 2 and Table 3.

Table 2. The first three non-dimensional transverse frequencies ($\mu_i=\omega_i\sqrt{\rho_0 A_0 l^4/E_0 I_0}$) of a tapered beam (NE=12)

	c	0.1	0.2	0.3	0.4	0.5	0.6	0.7	0.8	0.9
μ_1	Present	3.5587	3.60828	3.66675	3.73708	3.82379	3.93429	4.08171	4.2925	4.63073
	Attarnejad [31]	3.5587	3.60828	3.66675	3.73708	3.82379	3.93429	4.08173	4.29252	4.63079
	Banerjee *et al.* [15]	3.5587	3.60827	3.66675	3.73708	3.82379	3.93428	4.08171	4.29249	4.63073
μ_2	Present	21.3381	20.621	19.8806	19.1138	18.3173	17.4879	16.6253	15.7428	14.931
	Attarnejad [31]	21.3385	20.6214	19.881	19.1142	18.3177	17.4884	16.6259	15.7437	14.9332
	Banerjee *et al.* [15]	21.3381	20.621	19.8806	19.1138	18.3173	17.4878	16.6252	15.4727	14.9308
μ_3	Present	58.9804	56.1927	53.3227	50.3541	47.2653	44.0253	40.5884	36.8853	32.8346
	Attarnejad [31]	58.9874	56.1996	53.3294	50.3609	47.2722	44.0326	40.5966	36.8957	32.8538
	Banerjee *et al.* [15]	58.9799	56.1923	53.3222	50.3537	47.2649	44.0248	40.5879	36.8846	32.8331

Table 3. The first three non-dimensional transverse frequencies ($\mu_i = \omega_i \sqrt{\rho_0 A_0 l^4 / E_0 I_0}$) of a tapered beam (NE=12)

	c	0.1	0.2	0.3	0.4	0.5	0.6	0.7	0.8	0.9
μ_1	Present	3.6737	3.85512	4.06693	4.31878	4.62515	5.00903	5.50926	6.1964	7.20488
	Attarnejad [31]	3.6737	3.85512	4.06694	4.31878	4.62516	5.00905	5.50929	6.19646	7.20506
	Banerjee *et al.* [15]	3.6737	3.85511	4.06694	4.31878	4.62515	5.00904	5.50926	6.19639	7.20488
μ_2	Present	21.5503	21.0568	20.5555	20.05	19.5476	19.0649	18.6412	18.3856	18.6805
	Attarnejad [31]	21.5506	21.0571	20.5559	20.0505	19.5482	19.0656	18.6422	18.3872	18.6848
	Banerjee *et al.* [15]	21.5503	21.0568	20.5555	20.05	19.5476	19.0649	18.6412	18.3855	18.6803
μ_3	Present	59.1891	56.6308	54.0157	51.3351	48.5794	45.7389	42.8111	39.8346	37.1261
	Attarnejad [31]	59.1962	56.6379	54.0227	51.3423	48.587	45.7472	42.8209	39.8485	37.1573
	Banerjee *et al.* [15]	59.1886	56.6303	54.0152	51.3346	48.5789	45.7384	42.8104	39.8336	37.1241

Table 4 is tabulated for fourth and fifth natural frequencies and specified taper ratio c=0.5.

Table 4. The effect of this element on higher frequencies

	n=1		**n=2**	
	μ_4	μ_5	μ_4	μ_5
Present(NE=12)	90.4537	148.016	91.8162	149.404
Banerjee *et al.* [15]	90.4505	148.002	91.8128	149.39

The effect of this element on taper ratios higher than 0.9 are presented in Table 5.

Table 5. The effect of this element on higher taper ratios

		n=1		**n=2**	
	NE=20	**c=0.99**	**c=0.995**	**c=0.99**	**c=0.995**
μ_1	Present	5.21446	5.26321	8.54601	8.62732
	Banerjee *et al.* [15]	5.21445	5.26337	8.54601	8.63232
μ_2	Present	14.9672	15.0708	20.7302	20.8613
	Banerjee *et al.* [15]	14.967	15.0722	20.7301	20.9355
μ_3	Present	29.7292	29.8062	37.7284	37.7216
	Banerjee *et al.* [15]	29.7265	29.8064	37.7253	38.0742
μ_4	Present	49.7144	49.5695	59.6492	59.2879
	Banerjee *et al.* [15]	49.6986	49.5473	59.6278	60.0908

Example 2.

Consider a beam of constant depth whose cross-sectional area and moment of inertia respectively vary as:

$A = e^{\delta\xi}$,$I = e^{\delta\xi}$

The first three natural frequencies for SS and CC boundary conditions and a given non-uniformity parameter, δ , are determined and compared with those of Ece et al. [12]. Furthermore, the first five natural frequencies for CF boundary condition and non-uniformity parameter $\delta = -1$, are determined and compared with those of Attarnejad et al. [37]. Cranch and Adeer [39]. Ece et al. [12] and Tong and Tabarrok [40]. The results are tabulated in Table 6 and Table 7.

Table 6. The effect of number of elements on accuracy of dimensionless natural frequencies for and different taper ratios and boundary conditions

δ	Mode number	SS			CC		
		Present		Ece *et al.* [12]	Present		Ece *et al.* [12]
		NE=10	NE=20		NE=10	NE=20	
0	1	9.86961	9.8696	9.8696	22.37333	22.37329	22.37327
	2	39.47868	39.47843	39.47841	61.673838	61.67289	61.67281
	3	88.82946	8.882663	88.82643	120.91101	120.90387	120.90338
	4	157.93057	157.91474	157.91367	199.89368	199.86161	199.85945
	5	246.80417	246.74416	246.74011	298.6689	298.56272	298.55552
1	1	9.77291	9.77291	9.77291	22.51173	22.51168	22.51167
	2	39.57063	39.57038	39.57036	61.86072	61.85976	61.85968
	3	88.97356	88.97071	88.97052	121.11564	121.10847	121.10799
	4	158.10114	158.08526	158.08418	200.10846	200.07628	200.07411
	5	246.99071	246.93057	246.9265	298.89023	298.78382	298.77661

Table 7. Dimensionless natural frequencies of the beam in Example 2 (δ= -1).

Mode number	Present (NE=20)	Attarnejad *et al.* [37]	Cranch and Adler [39]	Tong and Tabarrok [40]	Ece *et al.* [12]
1	4.7349	4.7349	4.735	4.7347	4.72298
2	24.20187	24.2018	24.2025	24.2005	24.20168
3	63.86561	63.8645	63.85	63.8608	63.86448
4	123.10588	123.098	-	123.91	123.0979
5	202.10378	-	-	-	202.0687

Tables 2 to 7 show that the predicted results by the present element are in good agreement with results obtained from previous method. In example 1, unlike the first mode the second and third modes decrease with increased taper ratio, which is due to the softening effect resulting from the reduction in cross-sectional area and moment of inertia. It is worth mentioning that with the equal number of elements, 3-node method yields more accurate results than 2-node method. In example 1 and 2, the results are acceptable for taper ratios upper than 0.9, higher frequencies and different boundary conditions. Figure 7 is plotted in order to show the effects of taper ratios on all six shape functions. It is observed that the effect of taper ratio is clearly reflected in shape functions.

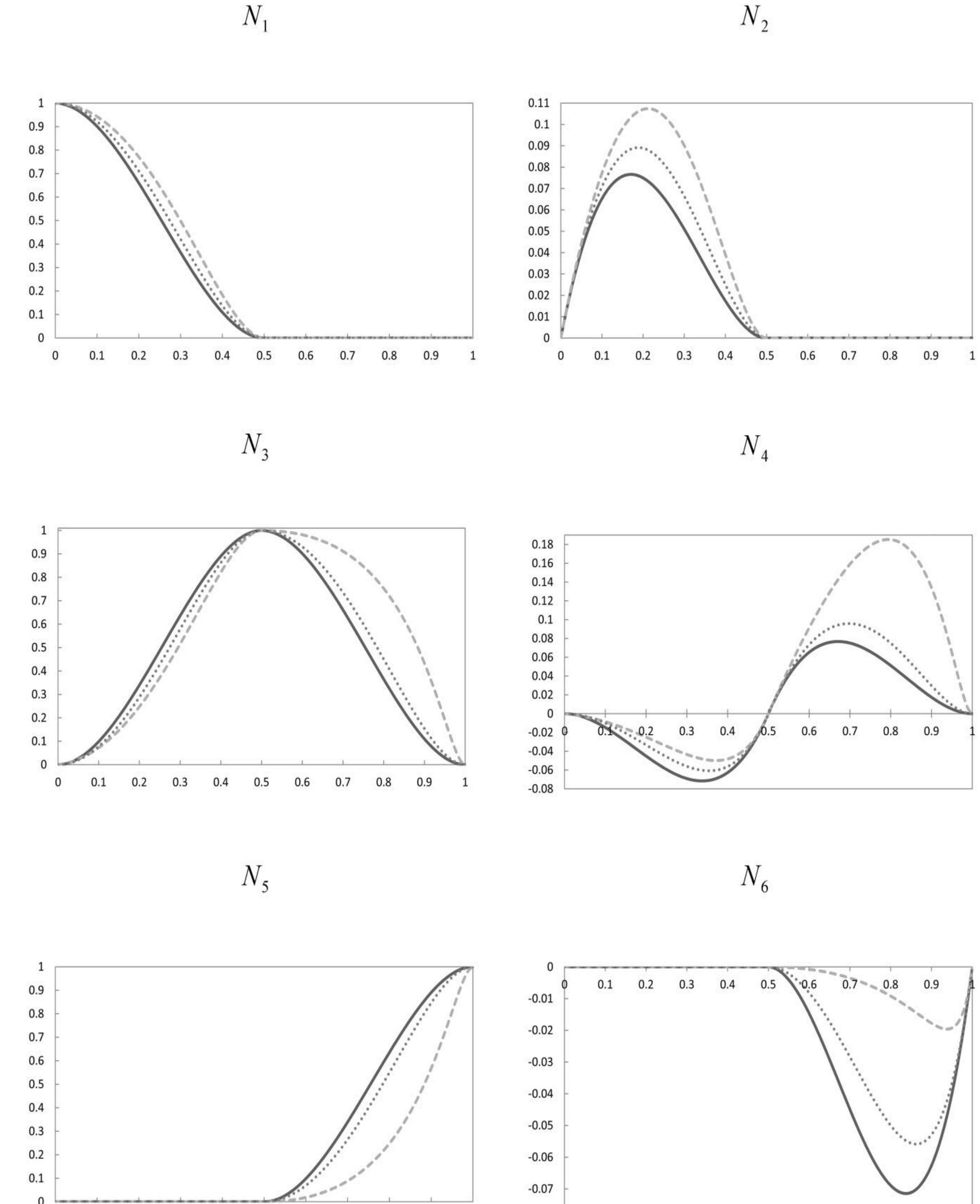

Fig. 7. Variation of shape function of beam element of unit length for example 1 and n=2 (solid line: C=0.1, Dotted line C=0.5, Dashed line: C=0.9)

In order to compare convergence between 3-node method and 2-node method, Figure 8 are plotted for a cantilever beam with $A = e^{0.5\xi}$, $I = e^{0.5\xi}$

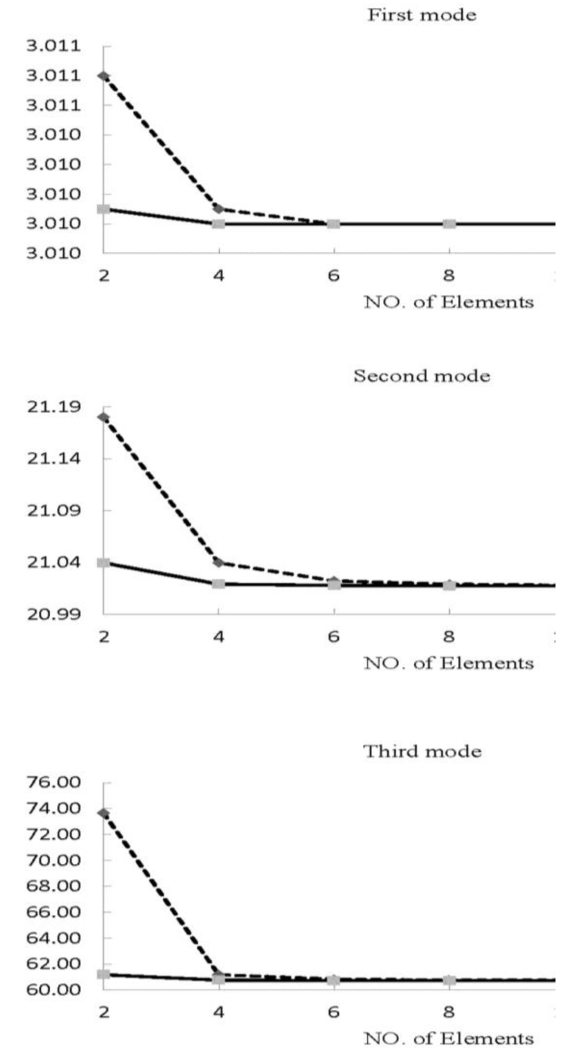

Fig. 8. Convergence of non-dimensional transverse frequencies of cantilever beam (0.5) and compare with 2-node method (solid line: 3-node, Dashed line: 2-node)

It is observed that utilizing fewer numbers of elements in 3-node method, the speed of convergence increases remarkably.

The results obtained from Banerjee *et al*. [15] are assumed as exact solution to calculate the error. Figure 9 illustrates the error concerning of third mode frequency in example 2. The figure indicates that as the number of elements and taper ratio increase, the errors are in a similar range and consequently, the element stays stable.

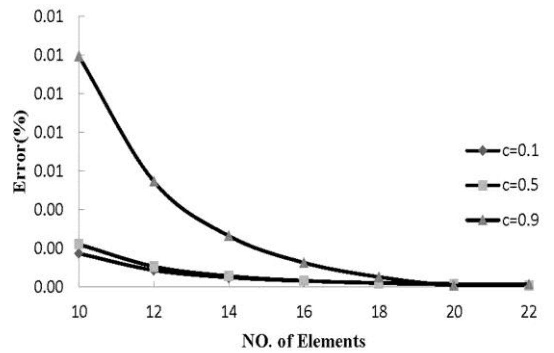

Fig. 9. Error concerning of third mode frequency with respect to number of elements

Finally, benchmark example is provided. In this example, it is assumed that

$$A(\xi) = A_0\left(1-c_b\xi\right)\left(1-c_h\xi\right)^2$$

$$I(\xi) = I_0\left(1-c_b\xi\right)\left(1-c_h\xi\right)^4$$

where c_b and c_h are taper ratios. In order to facilitate the presentation of benchmark results, non-dimensional parameters are introduced in Table 8.

Table 8. First three non-dimensional transverse frequencies of non-prismatic Euler-Bernoulli beam

		C_b	0			0.3			0.6			0.9		
	NE	C_h	μ_1	μ_2	μ_3	μ_1	μ_2	μ_3	μ_1	μ_2	μ_3	μ_1	μ_2	μ_3
S-S	10	0	9.8696	39.4787	88.8295	9.8574	39.4899	88.8474	9.7946	39.5384	88.9357	9.5441	39.5586	89.1311
		0.3	8.2502	33.4015	75.712	8.1783	33.4706	75.1792	8.0337	33.6009	75.3938	7.6541	33.7651	75.8167
		0.6	6.2086	26.852	59.9938	6.0815	26.9886	60.1969	5.8609	27.224	60.5545	5.3579	27.6062	61.2759
		0.9	3.0513	19.0941	41.4977	2.9038	19.3619	41.8282	2.6604	19.8372	42.4141	2.1299	20.8582	43.805
	20	0	9.8696	39.4784	88.8266	9.8574	39.4896	88.8446	9.7946	39.5382	88.9328	9.5441	39.5584	89.1283
		0.3	8.2502	33.4013	75.0687	8.1783	33.4704	75.1767	8.0337	33.6007	75.3913	7.6541	33.7649	75.8141
		0.6	6.2086	26.8518	59.9915	6.0815	26.9884	60.1945	5.8609	27.2238	60.5521	5.3579	27.606	61.2734
		0.9	3.0513	19.0938	41.494	2.9038	19.3616	41.8245	2.6604	19.8368	42.4103	2.1299	20.8579	43.8008
C-C	10	0	22.3733	61.6738	120.911	22.3213	61.6028	120.8329	22.0465	61.2143	120.3964	20.784	59.168	117.8486
		0.3	18.9233	52.0864	102.05	18.9974	52.1866	102.16	18.9399	52.1027	102.0642	18.1829	50.8513	100.4863
		0.6	15.1898	41.4773	80.9834	15.4008	41.7544	81.2861	15.5863	41.9997	81.5565	15.4136	41.658	81.0894
		0.9	10.7636	28.2362	54.1083	11.1752	28.719	54.6245	11.7312	29.3891	55.3494	12.4914	30.4	56.4982

Table 8. First three non-dimensional transverse frequencies of non-prismatic Euler-Bernoulli beam (continue)

	NE	C_b	0			0.3			0.6			0.9		
		C_h	μ_1	μ_2	μ_3	μ_1	μ_2	μ_3	μ_1	μ_2	μ_3	μ_1	μ_2	μ_3
C-C	20	0	22.3733	61.6729	120.904	22.3213	61.6019	120.8258	22.0465	61.2134	120.3894	20.784	59.1671	117.842
		0.3	18.9232	52.0856	102.044	18.9974	52.1857	102.1539	18.9398	52.1019	102.058	18.1829	50.8506	100.4805
		0.6	15.1898	41.4766	80.9779	15.4007	41.7536	81.2805	15.5862	41.9989	81.5509	15.4135	41.6572	81.0838
		0.9	10.7636	28.2353	54.1012	11.1752	28.7181	54.6172	11.7312	29.3881	55.3417	12.4914	30.3989	56.4902
C-F	10	0	3.516	22.0345	61.6982	3.916	22.786	62.4372	4.5853	24.0211	63.7526	6.0704	27.299	68.1159
		0.3	4.0669	20.5556	54.0162	4.5004	21.2539	54.746	5.2231	22.4097	56.0114	6.8148	25.5282	60.0635
		0.6	5.009	19.065	45.7396	5.4889	19.7173	46.4495	6.2816	20.8063	47.6543	7.994	23.7956	51.3851
		0.9	7.2049	18.6808	37.1285	7.7631	19.3087	37.8012	8.6463	20.3767	38.946	10.388	23.3075	42.4561
	20	0	3.516	22.0345	61.6973	3.916	22.786	62.4362	4.5853	24.0211	63.7515	6.0704	27.2989	68.1146
		0.3	4.0669	20.5555	54.0153	4.5004	21.2538	54.745	5.2231	22.4096	56.0104	6.8148	25.5281	60.0622
		0.6	5.009	19.0649	45.7384	5.4889	19.7172	46.4483	6.2816	20.8062	47.6531	7.994	23.7955	51.3834
		0.9	7.2049	18.6802	37.1241	7.763	19.3081	37.7965	8.6462	20.376	38.9409	10.3879	23.3065	42.4494
C-S	10	0	15.4182	49.9654	104.253	15.7687	50.2939	104.5828	16.1948	50.7029	105.0124	16.6372	51.1485	105.6097
		0.3	13.9617	43.1283	88.9422	14.2939	43.5113	89.3501	14.7019	44.0033	89.8955	15.1302	44.6113	90.7173
		0.6	12.2329	35.5595	71.8982	12.5739	35.9984	72.3812	13.0088	36.5866	73.05	13.5171	37.4217	74.1576
		0.9	9.9086	26.1094	50.3911	10.353	26.632	50.9559	10.9793	27.3998	51.8011	11.9495	28.8143	53.5177
	20	0	15.4182	49.9649	104.248	15.7686	50.2934	104.5782	16.1948	50.7024	105.0077	16.6372	51.1479	105.605
		0.3	13.9617	43.1279	88.9381	14.2939	43.5108	89.3459	14.7019	44.0028	89.8912	15.1302	44.6108	90.7129
		0.6	12.2328	35.559	71.8942	12.5738	35.9979	72.3771	13.0087	36.5861	73.0458	13.517	37.4211	74.1532
		0.9	9.9086	26.1087	50.3846	10.353	26.6311	50.9491	10.9793	27.3989	51.794	11.9495	28.8133	53.51

5. Conclusions

A flexibility-based method for static and dynamic analysis of non-prismatic Euler-Bernoulli beams has been presented. The main aspects of new approach are:

1. Introduction of 3-node BDFs.
2. All types of cross-sections and cross-sectional dimensions of the beam element could be considered in this method.
3. Shape functions for any type of cross sectional properties could be obtained for that type.
4. Although the new shape functions are derived based on static deformations, they were employed in the dynamic analysis, satisfactory results were obtained for natural frequencies even for a coarse mesh.
5. The new element provides better results with the same mesh in upper frequencies and different boundary conditions than 2-node element.
6. The method can be extended to analysis of curved beams as well as shells of revolution.
7. The method can be used for analysis of straight and curved Timoshenko beam elements.
8. The method is being extended to analysis of plates and shells.

Appendix A

Heaviside step function was defined as:

$$H(y) = \begin{cases} 0 & y < 0 \\ \dfrac{1}{2} & y = 0 \\ 1 & y > 0 \end{cases}$$

References

[1]. Gunda J.B., Ganguli R., 2008, New rational interpolation functions for finite element analysis of rotating beams, Int. J. Mech. Sci. **50:** 578-588.

[2]. Caruntu D.I., 2009, Dynamic modal characteristics of transverse vibrations of cantilevers of parabolic thickness, Mech. Res. Commun. **36:** 391–404.

[3]. Gallagher R.H., Lee C.H., 1970, Matrix dynamic and instability analysis with non-uniform elements, J. Numer. Meth. Eng. **2:** 265-275.

[4]. Karabalis D.L., Beskos D.E., 1983, Static, dynamic and stability analysis of structures

composed of tapered beams, Comput. Struct. **16:** 731-748.

[5]. Eisenberger M., Reich Y., 1989, Static, vibration and stability analysis of non-uniform beams, Comput. Struct. **31:** 563-571.

[6]. Eisenberger M., 1986, An exact element method, Int. J. Numer. Meth. Eng. **30:** 363-370.

[7]. Eisenberger M., 1991, Exact solution for general variable cross-section members, Comput. Struct. **41:** 765-772.

[8]. Banerjee J.R., Williams F.W., 1985, Exact Bernoulli-Euler dynamic stiffness matrix for a range of tapered beam, J. Numer. Meth. Eng. **21:** 2289-2302.

[9]. Mou Y., Han R.S.P., Shah A.H., 1997, Exact dynamic stiffness matrix for beams of arbitrarily varying cross sections, Int. J. Numer. Meth. Eng. **40:** 233-250.

[10]. Chambers J.J., Almudhafar S., Stenger F., 2003, Effect of reduced beam section frame elements on stiffness of moment frames, J. Struct. Eng. **129:** 383-393.

[11]. Kim K.D., Engelhardt M.D., 2007, Nonprismatic beam element for beams with RBS connections in steel moment frames, J. Struct. Eng. **133:** 176-184.

[12]. Ece M.C., Aydogdu M., Taskin V., 2007, Vibration of a variable cross-section beam, Mech. Res. Commun. **34:** 78-84.

[13]. Banerjee J.R., 2000, Free vibration of centrifugally stiffened uniform and tapered beams using the dynamic stiffness method. J. Sound Vib. **233:** 857-875.

[14]. Wang G., Wereley N.M., 2004, Free vibration analysis of rotating blades with uniform tapers, J. AIAA **42:** 2429-2437.

[15]. Banerjee J.R., Su H., 2006, Jackson D.R., Free vibration of rotating tapered beams using the dynamic stiffness method, J. Sound Vib. **298:** 1034-1054.

[16]. Ruta P., 1999, Application of Chebyshev series to solution of non-prismatic beam vibration problems, J. Sound Vib. **227:** 449-467.

[17]. Auciello N.M., Ercolano A., 2004, A general solution for dynamic response of axially loaded non-uniform Timoshenko beams, Int. J. Solids Struct. **41:** 4861–4874.

[18]. Ho S.H., Chen C.K., 1998, Analysis of general elastically end restrained non-uniform beams using differential transform, Appl. Math. Model. **22:** 219–234.

[19]. Zeng H., Bert C.W., 2001, Vibration analysis of a tapered bar by differential transformation, J. Sound Vib. **242:** 737–739.

[20]. Ozdemir O., Kaya M.O., 2006, Flapwise bending vibration analysis of a rotating tapered cantilever Bernoulli–Euler beam by differential transform method, J. Sound Vib. **289:** 413–420.

[21]. Ozdemir O., Kaya M.O., 2006, Flapwise bending vibration analysis of double tapere rotating Euler–Bernoulli beam by using the differential transform method, Meccanica **40:** 661–670.

[22]. Seval C., 2008, Solution of free vibration equations of beam on elastic soil by using differential transform method, Appl. Math. Model **32:** 1744-1757.

[23]. Balkaya M., Kaya M.O., Saglamer A., 2009, Analysis of the vibration of an elastic beam supported on elastic soil using the differential transform method, Arch. Appl. Mech. **79:** 135–146.

[24]. Catal S., 2008, Solution of free vibration equations of beam on elastic soil by using differential transform method, Appl. Math. Model. **32:** 1744–1757.

[25]. Yesilce Y., Catal S., 2009, Free vibration of axially loaded Reddy-Bickford beam on elastic soil using the differential transform method, Struct. Eng. Mech. **31:** 453–476.

[26]. Yesilce Y., 2010, DTM and DQEM for free vibration of axially loaded and semi-rigid-connected Reddy-Bickford beam, Commun. Numer. Meth. Eng. **27:** 666-693.

[27]. Attarnejad R., Shahba A., 2008, Application of differential transform method in free vibration analysis of rotating non-prismatic beams, World Appl. Sci. J. **5:** 441-448.

[28]. Shahba A., Rajasekaran S., 2012, Free vibration and stability of tapered Euler-Bernoulli beams made of axially functionally graded materials, Appl. Math. Model. **36:** 3094-3111.

[29]. Attarnejad R., 2000, On the derivation of the geometric stiffness and consistent mass matrices for non-prismatic Euler-Bernoulli beam elements, Barcelona, Proceedings of European Congress on Computational Methods in Applied Sciences and Engineering.

[30]. Attarnejad R., 2002, Free vibration of non-prismatic beams, New York, Proceedings of 15th ASCE Engineering Mechanics Conference.

[31]. Attarnejad R., 2010, Basic displacement functions in analysis of non-prismatic beams, Eng. Comput. **27:** 733-776.

[32]. Attarnejad R., Shahba A., 2011, Basic displacement functions in analysis of centrifugally stiffened tapered beams, AJSE **36:** 841-853.

[33]. Attarnejad R., Shahba A., Semnani S.J., 2011, Analysis of non-prismatic Timoshenko beams using basic displacement functions, Adv. Struct. Eng. **14:** 319-332.

[34]. Attarnejad R., Shahba A., 2010, Dynamic basic displacement functions in free vibration analysis of centrifugally stiffened tapered

beams; a mechanical solution, Meccanica **46:** 1267-1281.

[35]. Attarnejad R., Shahba A., 2011, Basic displacement functions for centrifugally stiffened tapered beams, Commun. Numer. Meth. Eng. **27:** 1385-1397.

[36]. Attarnejad R., Semnani S.J., Shahba A., 2010, Basic displacement functions for free vibration analysis of non-prismatic Timoshenko beams, Finite Elem. Anal. Des. **46:** 916-929.

[37]. Attarnejad R., Shahba A., Eslaminia M., 2011, Dynamic basic displacement functions for free vibration analysis of tapered beams, J. Vib. Control **17:** 2222-2238.

[38]. Franciosi C., Mecca M., 1998, Some finite elements for the static analysis of beams with varying cross section, Comput. Struct. **69:** 191-196.

[39]. Cranch E.T., Adler A.A., 1956, Bending vibration of variable section beams, J. Appl. Mech. **23:** 103–108.

[40]. Tong X., Tabarrok B., 1995, Vibration analysis of Timoshenko beams with non-homogeneity and varying cross-section, J. Sound Vib. **186:** 821–835.

Nomenclature

l beam length

$b_{u1}, b_{w1}, b_{\theta1}, b_{u2}, b_{w2}, b_{\theta2}, b_{u3}, b_{w3}, b_{\theta3}$ basic displacement functions

μ_i non-dimensional transverse natural frequencies

c taper ratio

$\mathbf{F_{11}}$ nodal flexibility matrix of the left node

$\mathbf{F_{22}}$ nodal flexibility matrix of the mid node

$\mathbf{F_{33}}$ nodal flexibility matrix of the right node

x longitudinal coordinate

NE total number of beam elements

I_0 moment of inertia at origin

$\mathbf{b}'_w, \mathbf{b}''_\mathbf{w}$ first and second derivative of $\mathbf{b_w}$ with respect to x

$\mathbf{K_{11}}$ nodal stiffness matrix of the left node

$\mathbf{K}_{22}$ nodal stiffness matrix of the mid node

$\mathbf{K}_{33}$ nodal stiffness matrix of the right node

$\mathbf{F}$ equivalent nodal forces

$\mathbf{G}$ matrix containing nodal flexural stiffness matrices

E_0 modulus of elasticity at origin

ρ_0 mass density at origin

A_0 cross-sectional area at origin

$\mathbf{M}$ element consistent mass matrix

$\mathbf{N}$ shape functions

$\mathbf{N}', \mathbf{N}''$ first and second derivative of $\mathbf{N}$ with respect to x